

Video Article

Athymic Rat Model for Evaluation of Engineered Anterior Cruciate Ligament Grafts

Natalie L. Leong¹, Nima Kabir¹, Armin Arshi¹, Azadeh Nazemi², Ben M. Wu², David R. McAllister¹, Frank A. Petrigliano¹

¹Department of Orthopaedic Surgery, University of California Los Angeles

²Department of Bioengineering, University of California Los Angeles

Correspondence to: Natalie L. Leong at NLeong@mednet.ucla.edu

URL: <https://www.jove.com/video/52797>

DOI: [doi:10.3791/52797](https://doi.org/10.3791/52797)

Keywords: Bioengineering, Issue 97, Anterior cruciate ligament, tissue engineering, animal model, biodegradable scaffold, rat, knee

Date Published: 3/26/2015

Citation: Leong, N.L., Kabir, N., Arshi, A., Nazemi, A., Wu, B.M., McAllister, D.R., Petrigliano, F.A. Athymic Rat Model for Evaluation of Engineered Anterior Cruciate Ligament Grafts. *J. Vis. Exp.* (97), e52797, doi:10.3791/52797 (2015).

Abstract

Anterior cruciate ligament (ACL) rupture is a common ligamentous injury that often requires surgery because the ACL does not heal well without intervention. Current treatment strategies include ligament reconstruction with either autograft or allograft, which each have their associated limitations. Thus, there is interest in designing a tissue-engineered graft for use in ACL reconstruction. We describe the fabrication of an electrospun polymer graft for use in ACL tissue engineering. This polycaprolactone graft is biocompatible, biodegradable, porous, and is comprised of aligned fibers. Because an animal model is necessary to evaluate such a graft, this paper describes an intra-articular athymic rat model of ACL reconstruction that can be used to evaluate engineered grafts, including those seeded with xenogeneic cells. Representative histology and biomechanical testing results at 16 weeks postoperatively are presented, with grafts tested immediately post-implantation and contralateral native ACLs serving as controls. The present study provides a reproducible animal model with which to evaluate tissue engineered ACL grafts, and demonstrates the potential of a regenerative medicine approach to treatment of ACL rupture.

Video Link

The video component of this article can be found at <https://www.jove.com/video/52797/>

Introduction

Rupture of the anterior cruciate ligament (ACL) is one of most common ligament injuries of the knee¹. Because the ruptured ACL's is unable to heal without surgical intervention, the limitations in activities of daily living as well as participation in sports drive over 175,000 patients to undergo surgery each year², with an estimated cost of one billion dollars annually³. Currently, either autograft or allograft tendon is used for ligament reconstruction. Though high success rates can be achieved with both autograft and allograft replacement, serious complications are associated with these reconstruction options⁴. Autograft tissue is associated with donor site morbidity and is limited in supply, especially in instances of re-rupture or multi-ligamentous injury. On the other hand, allograft tissue is linked with delayed graft integration, adverse inflammatory response, theoretical infectious risk, and limited supply⁵. Synthetic non-degradable grafts were developed in the 1970s and 1980s but were hampered by premature graft rupture, foreign body reactions, osteolysis, and synovitis⁶. As a result of these serious concerns, there are currently no synthetic grafts available for clinical use in the United States.

Due to these limitations with existing graft options and to recent developments in biology, engineering, and regenerative medicine, there has been great interest in a tissue engineered solution for ACL grafting. Current tissue engineering strategies employ degradable biological and synthetic materials to allow for host tissue ingrowth while avoiding the limitations associated with permanent synthetic material implantation⁷.

Polycaprolactone (PCL) is a biodegradable polymer that is FDA approved for a number of medical applications including adhesion barrier and wound dressing⁸, that has been used in a wide variety of applications including vascular, bone, cartilage, nerve, skin, and esophageal tissue engineering^{5,9-16}. Favorable biocompatibility, relatively long *in-vivo* half-life, adequate mechanical strength, and high elasticity contribute to the popularity of this polymer in tissue engineering. In a rodent model of wound healing, implanted electrospun PCL was shown to be non-immunogenic and to integrate into local tissue without adverse reactions¹³. An SEM image of electrospun PCL is shown in **Figure 1**.

With current FDA regulatory standards, efficacy and safety in both small and large animal models would be required for a PCL or any other engineered ACL graft to move into clinical trials in the United States. Additionally, *in vivo* conditions can often augment the properties of an *in vitro* tissue engineered ACL graft. A rat model of autologous ACL reconstruction with flexor digitorum longus tendon has been previously described, in which the native ACL was severed, femoral and tibial tunnels were drilled, and the graft was passed and secured in place with suture¹⁷⁻²². In this paper, we will describe a modification of this model for the evaluation of engineered ACL replacements rather than for autograft-based reconstruction (**Figure 2**).

Although many animal models exist for ligament tissue engineering, the rat is advantageous compared to larger models for a number of reasons. These advantages include easier husbandry and handling, fewer ethical considerations, and reduced cost^{17,23}. In addition, the rat model has

been used extensively as a model for orthopaedic tissue regeneration, including cartilage, tendon, and bone tissue engineering²⁴. In particular, athymic nude rats were chosen due to their lack of cell-mediated immune response²⁵, allowing for the eventual implantation of xenogeneic donor cells in this model to further enhance the engineered graft in the future. In this methods paper, we describe the fabrication and surgical implantation of an acellular, biodegradable polymer graft in an athymic rat model of ACL reconstruction.

Protocol

NOTE: All animal surgeries were approved by the local veterinary staff and animal use committee prior to commencing the experiments.

1. Preparation of Electrospun Polycaprolactone Scaffolds

1. Weigh and dissolve medical grade ester terminated poly (ϵ -caprolactone) in granule form in 1,1,1,3,3,3-hexafluoro-2-propanol to create a 10% w/w solution of the PCL polymer. Let the solution stir using a stir plate for at least 3 hr to ensure a homogenous solution.
2. Electrospin the PCL solution to create a cuff of highly aligned PCL fibers for scaffold fabrication.
 1. Prepare the electrospinning setup in a chemical fume hood with the fan on at all times. This consists of a large acrylic box that will serve as an isolated vacuum medium for the electrospinning process and has entry points for the source PCL solution driven by a voltage source, the motor-powered collecting mandrel, and a vacuum port. Clean the acrylic box thoroughly with ethanol and cover all surfaces with Parafilm sheets to remove any impurities that may compromise the quality of the electrospun product.
 2. Load approximately 3 ml of the above solution into a 10 ml syringe with a blunt ended 18 G, 1 ½ inch needle. Remove any air bubbles by pushing the syringe up. Lock solution into a programmable syringe pump. Insert the needle through a small hole into the acrylic box while leaving about ½ inch of the needle outside of the acrylic box for attachment of the voltage source wire.
 3. Use a 30 mm rotating lathe mandrel as the collector for the highly aligned PCL fibers; cover the mandrel tightly with a thin strip of aluminum foil. Lock the mandrel into the motor on the opposite side of the box about 15 cm away from the syringe needle.
 4. Insert the plastic hose into the vacuum port and connect to the fume hood vacuum source. Turn on the vacuum source and cover the acrylic box with a lid.
 5. Set the infusion rate of the programmable syringe pump to 2.5 ml/hr. Turn on the motor to operate the mandrel at 3,450 rpm and attach the positive lead of the voltage source to the needle tip outside of the box using an alligator clip.
 6. Once infusion of the PCL solution has begun, turn on the voltage source and set to a 20 kV operating voltage.
 7. Infuse the solution for 12 min to create a homogenous cuff from 0.5 ml of the PCL solution.
NOTE: On average, each cuff has enough electrospun material to create two six-strip sheets, which can be used to create a total of three four-layered scaffolds.
3. Laser cut the PCL cuff to form multiple small sheets on a VersaLaser Cutter 2.3 operated at low-vacuum setting, 10.0 keV landing voltage, 6.4 mm working distance, and probe diameter of 3.0.
NOTE: In this example, a computer aided design was used to instruct the cutter to yield multiple sheets of 1.5 mm x 35 mm x 150 μ m scaffolds with evenly distributed 150 μ m diameter holes at 15% pore area.
4. Plasma etch the PCL scaffolds using a plasma cleaner to induce hydrophilicity of the PCL surface with ion acceleration. Set the vacuum to 450 mTorr and the treat the scaffolds for 30 sec at high power (29.6 W).
5. Bathe the scaffolds in 70% ethanol in a sterile environment.
6. Coat the individual scaffolds with collagen to facilitate cellular adhesion and proliferation *in vivo*.
 1. Create a collagen coating solution by diluting a 8:1:2.5 sterile solution of Purecol collagen 3 mg/ml standard solution, 10x PBS and 0.1 N NaOH 1:9 in 1x PBS at 4 °C. Mix thoroughly to ensure solution homogeneity.
 2. Coat individual 1.5 mm x 35 mm x 150 μ m scaffolds with a thin layer film of the above collagen solution. Allow to dry for 24 hr in a sterile environment.
7. Using 5-0 Vicryl sutures, stack and affix four individual 1.5 mm x 35 mm x 150 μ m scaffolds using a Krackow stitch to create a final 0.6 mm thick, multi-layered, collagen-coated scaffold that is ready for implantation.

2. Rat Surgery Protocol

1. Induce anesthesia by placing rat in inhalation chamber and delivering 2% isoflurane with 2 L/min oxygen. Confirm the rat is adequately anesthetized by applying pressure to hind foot and evaluating for any response.
2. On the non-sterile back table, subcutaneously inject 25 mg/kg ampicillin and 0.03 mg/kg buprenorphine.
3. Apply ophthalmic ointment to the eyes. Clip the fur from the operative hind limb and prep the surgical site with three alternating scrubs of chlorhexidine and 70% ethanol.
4. Transfer the rat to the operating table, on a heated pad to prevent hypothermia. Secure nose cone, and maintain anesthesia through the procedure with 2% isoflurane in 2 L/min oxygen, delivered nose cone. Drape in a sterile manner, leaving the operative limb exposed.
5. Before starting the surgery, first confirm adequate anesthetization by lack of a response to hind foot pressure.
6. Make a 2 cm long vertical incision medial to the knee, centered at the level of the patella. Retract the skin laterally until the incision is centered over the knee.
7. Use a scalpel to make a medial parapatellar arthrotomy by cutting just medial to the patella and extending proximally to the level of the musculotendinous junction of the quadriceps and distally to the level of the patellar tendon insertion on the tibial tubercle. Take care not to cut the patellar or quadriceps tendons.
8. Release patella laterally by making a 1 cm vertical incision through the knee capsule just lateral to the patellar tendon.
9. Ensure the knee is extended. Take a pair of fine scissors and pass under the patella from lateral to medial. Spread the scissors a couple times so that the extensor mechanism can be translated to either side.
10. While flexing the knee, translate the patella laterally to expose the inside of the knee joint. Ensure clear visualization of the intercondylar notch and femoral condyles. Using a scalpel, transect the ACL and PCL in the notch.

11. Load power drill with a 1.6 mm k-wire. Place k-wire tip on ACL origin in the intercondylar notch. Drill superolaterally and visualize the exit point on the lateral aspect of the femur, removing any soft tissue as necessary with a scalpel. Pass the k-wire in and out a few times to ensure clear passage for the graft.
12. Place the k-wire on the ACL footprint on the tibial plateau. Drill anterolaterally and visualize exit point on the anterolateral proximal tibia. Use scalpel to clear soft tissue as necessary so that the point where the k-wire exits the tibia is fully visualized.
13. Pass a shortened Keith needle (ideally no more than 2 inches long) through the femoral bone tunnel. Thread the two suture ends from one end of the graft through the eye of the Keith needle. Use the needle to pull one end of the graft through the femoral tunnel.
14. Repeat the prior step to pass the other end of the graft through the tibial tunnel.
15. Use 4-0 Vicryl suture to affix the femoral end of the graft to surrounding periosteum or other soft tissue with a figure-of-eight stitch. Manually tension the graft with the knee in extension. Affix the tibial end of the graft to surrounding periosteum or other soft tissue with a figure-of-eight stitch.
16. Use a scissor to cut off excess graft on both ends, leaving 1-2 mm on each end past the figure-of-eight stitch.
17. Extend the knee and reduce the patella. Using 4-0 vicryl, place a single figure-of-eight stitch to close the medial joint capsule, preventing lateral subluxation of the patella.
18. Close the skin with a running subcuticular 5-0 Monocryl or Vicryl suture, with care not to suture the underlying muscle or have any visible suture once the skin is closed.
19. Inject rats subcutaneously with buprenorphine every 12 hr for a total of three days postoperatively. Check surgical site for any drainage or wound dehiscence at the time of injection. Limping and some swelling are normal in the first few days after surgery, but promptly address any postoperative concerns in conjunction with veterinary staff. The animal may be return to social housing at 2 weeks postoperatively, when surgical incisions are completely healed.

3. Data Collection Protocol

1. At the time of sacrifice, asphyxiate rats individually in a closed CO₂ chamber followed by thoracotomy.
2. Harvest both the surgically reconstructed and contralateral limbs by separating at the hip joint.
 1. For the reconstructed limbs, remove all soft tissue, including the posterior cruciate ligament and the remnants from the surgically disrupted native ACL, by fine dissection to isolate only the femur, tibia, and graft.
 2. For the contralateral limbs, remove all soft tissue except the native ACL as well as the femur and tibia by fine dissection.
 3. Use a rotary tool such as Dremel, to remove all but ¼ to 1 cm of bone from each end of the femur-graft-tibia complex.
 4. During this process and throughout biomechanical testing, regularly and frequently spray the ligamentous regions with normal saline to prevent desiccation of the harvested knee which may falsely alter results.
3. For histological analysis, fix each knee individually in 4% paraformaldehyde solution at 25 °C for 48 hr. Next, submerge the knee in a solution of Immunocal reagent for complete decalcification; this process is dependent on the calcific contents of the sample and may take up to five days. Check individual samples daily to assess progress as incomplete decalcification can lower sample quality. Once complete, perform sectioning, slide mounting, and staining as desired.
4. Perform biomechanical testing to assess the functional capacity of the tissue engineered ligament.
 1. Secure the femur and tibia by wrapping 28 G galvanized steel wire around the epiphysis of each bone separately. This is to prevent inaccurate biomechanical testing data from premature tensile failure of the sample at the bone rather than at the ligament of interest.
 2. Pot the femur into a mixture of polymethylmethacrylate (PMMA) bone cement. To do this, mix the two cement components and immediately use the viscous mixture to secure the femur into the metal, completely encasing the diaphysis of the bone in the cemented pot with the epiphysis and attached ligament protruding freely. Allow spontaneous free radical polymerization to gradually transform the mixed viscous components to a doughy material and eventually into a solid hardened matrix.
NOTE: This process takes several minutes and can be monitored by manually assessing the temperature of a bolus made from the remaining cement; the temperature should transiently increase during the exothermic polymerization reaction and subside to RT after the material solidifies.
 3. Repeat the same process above for cementing the tibia, except while maintaining the knee ligament at 20° flexion for ideal mechanical testing.
 4. Mount the cemented femur-graft-tibia complex onto a tensile testing apparatus, and prepare to record load and displacement as a function of time from the beginning of tension to failure. In this example, we used an Instron Model 5564 with a 1 kN load cell.
 5. Pre-tension the graft to 2 N at a ramp rate of 0.5 N/min and then test the graft to failure at a strain rate of 0.5 mm/sec. During the process, be sure that the ligament is failing at the mid-substance and that the bony femur and tibia are secure and not prematurely failing, which may inaccurately assess biomechanical properties of the tested ligament.
 6. Use the generated load-displacement curves to compute the failure load and stiffness of the tested ligament.

Representative Results

In our experience of 92 rat surgeries by a single surgeon, mean operative time from incision to completion of wound was 16.9 min, with a standard deviation of 4.7 min. At the time of sacrifice, rats weighed 356 ± 23 g. All rats tolerated the surgery well, and experienced no complications. Immediately after surgery, the rats were noted to bear weight on the operative extremity, but exhibited a slight limp. By one week post-operatively, all rats were ambulating with no appreciable limp. The animals all gained weight steadily during the course of the study, with no observed abnormalities in feeding, urination, or defecation habits. Clinically, no gross wound dehiscence, erythema, swelling, effusion, or drainage was observed postoperatively.

The 92 rat surgeries mentioned above were not performed primarily for the purpose of this methods manuscript. Rather, they were used to test various engineered graft conditions. While the detailed mechanical testing and histological results are outside the scope of this paper, more details can be found in a paper by Leong *et al.*²⁶. In brief, at 16 weeks following the reconstruction, histological analysis of the sectioned knee demonstrated that the scaffold matrix became largely infiltrated by fibroblasts secreting eosinophilic collagen with good integration into the

bone tunnels (**Figure 3**). At this time, the scaffold has been completely resorbed and no evidence of the polymer was visualized. Additionally, immunohistochemistry for the macrophage marker CD68 demonstrated minimal inflammatory response at 16 weeks post-operatively (**Figure 4**).

Biomechanical properties were assessed immediately after sacrifice. All tested samples failed at the mid-substance (**Figure 5**). Using load-displacement curves generated from tensile testing (**Figure 6**), failure load and stiffness were computed for each group. At 16 weeks post-implantation, the electrospun polymer graft had approximately double the peak load and stiffness of the graft tested immediately post-implantation, but these values were lower than the native ACL²⁶.

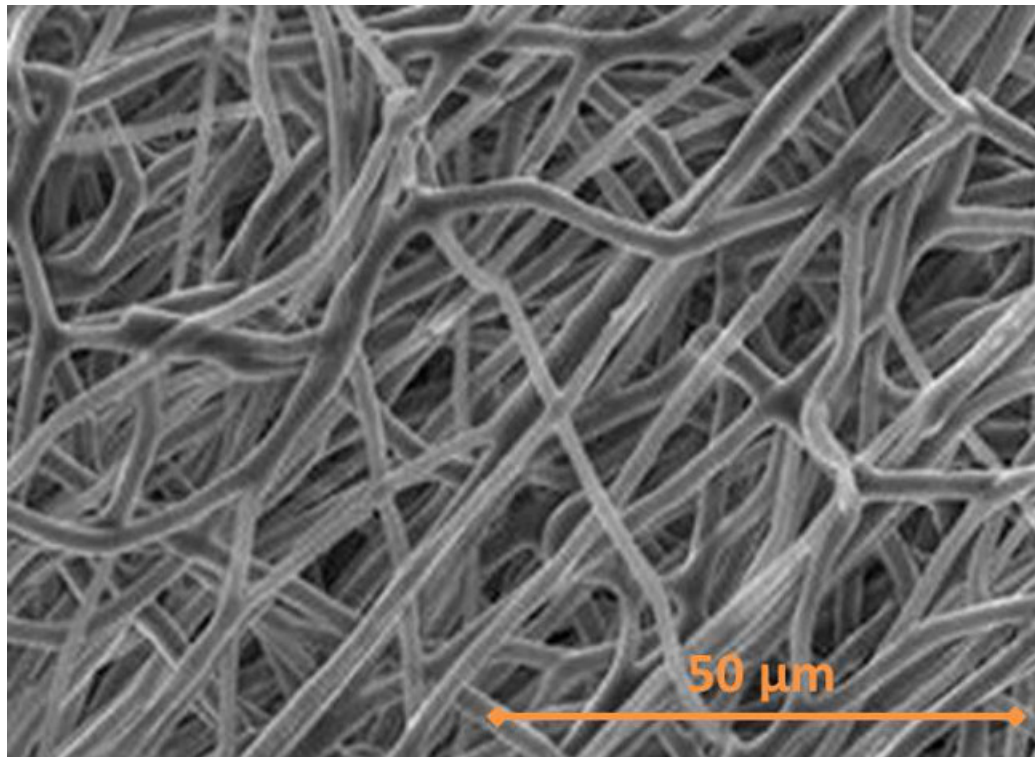


Figure 1. SEM image of electrospun polycaprolactone scaffold with aligned fibers. [Please click here to view a larger version of this figure.](#)

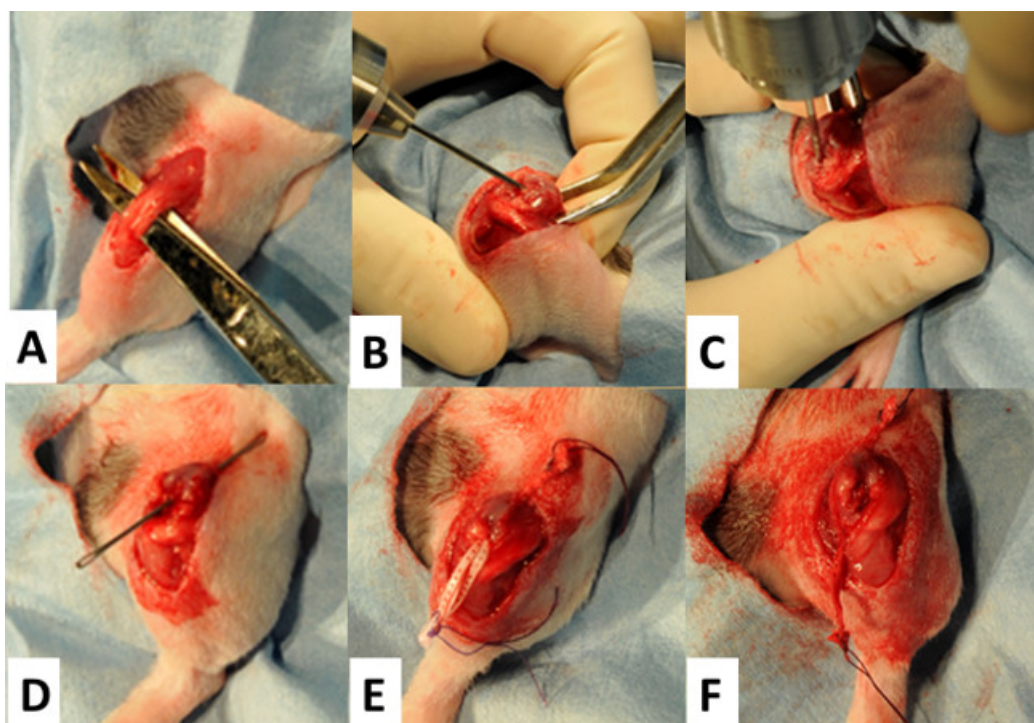


Figure 2. Athymic rat model of ACL reconstruction. (A) Isolation of the patellar tendon via a medial parapatellar skin incision. (B) Drilling of femoral tunnel using 1.6 mm k-wire. (C) Drilling of tibial tunnel. (D) Placement of 1.2 mm Keith needle through femoral tunnel to pull graft through. (E) Electrospun polycaprolactone graft pulled through femoral tunnel. (F) Graft pulled through both femoral and tibial tunnels, before the ends are trimmed and sutured to periosteum, and a layered closure is performed. [Please click here to view a larger version of this figure.](#)

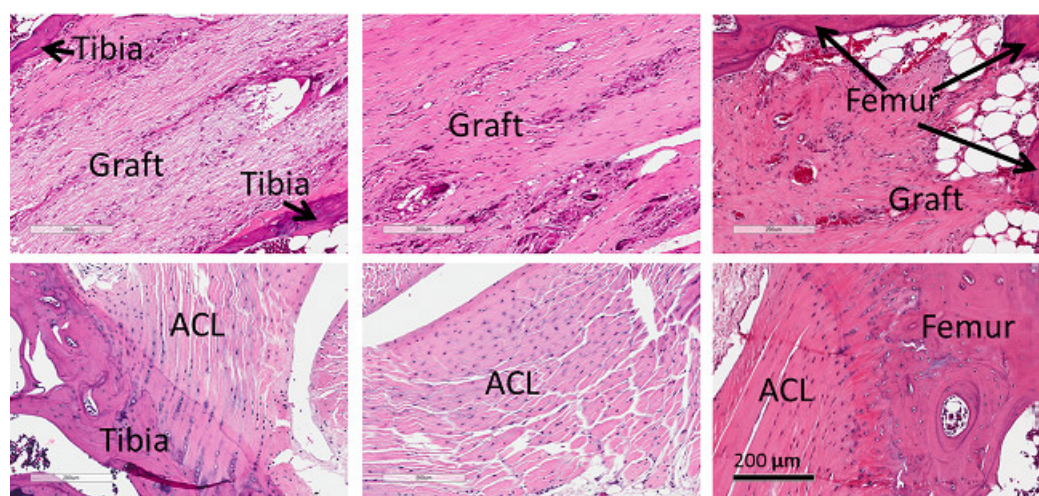


Figure 3. Hematoxylin and eosin staining of electrospun polymer graft (top) at tibial bone tunnel (left), midsubstance (center), and femoral bone tunnel (right). For comparison, native ACL is shown (bottom), at tibial insertion (left), midsubstance (center) and femoral origin (right), 10X. [Please click here to view a larger version of this figure.](#)

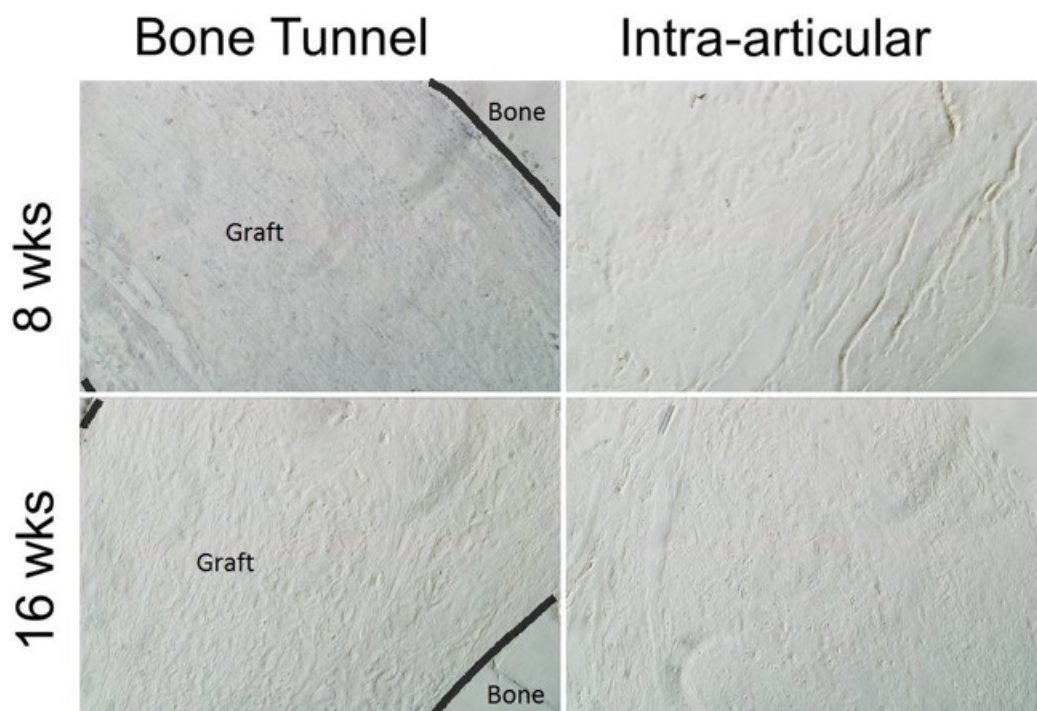


Figure 4. Colorimetric immunohistochemistry staining for CD68, a marker for macrophages. Qualitatively, there appears to be slightly more positive staining in the bone tunnel at 8 weeks than in the intra-articular region of the graft or at 16 weeks post-op. There appears to be minimal inflammation in the grafts. All images are 20X magnification. [Please click here to view a larger version of this figure.](#)

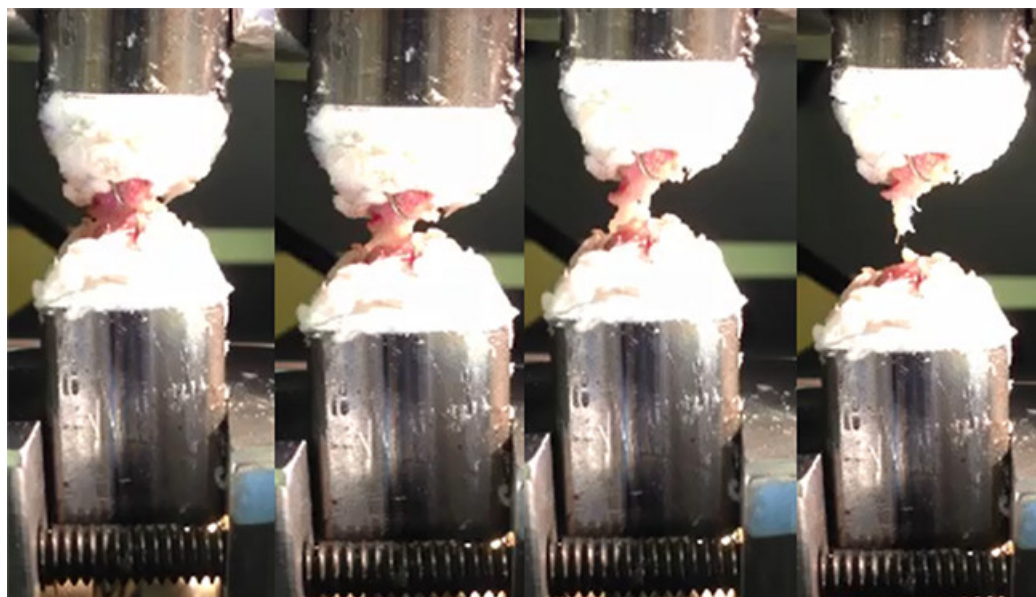


Figure 5. Images of mechanical testing of implanted electrospun graft, demonstrating failure at midsubstance of graft. [Please click here to view a larger version of this figure.](#)

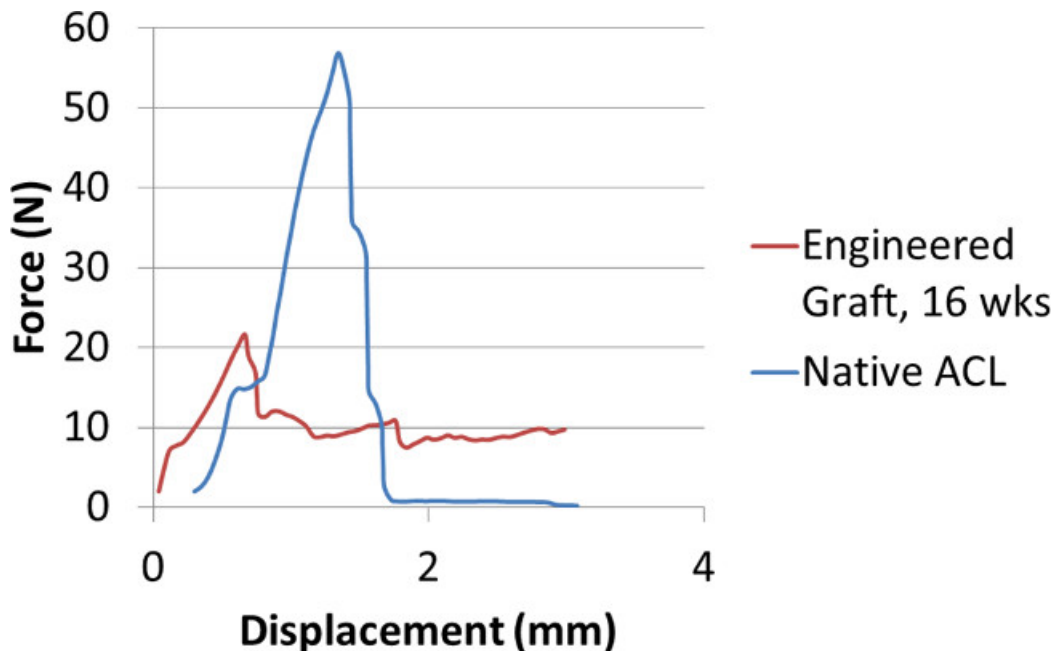


Figure 6. Sample load-displacement curve for tissue-engineered ACL graft at 16 weeks after implantation in athymic rat model. [Please click here to view a larger version of this figure.](#)

Discussion

ACL injuries are a common condition in orthopaedic sports surgery, with limited options for reconstruction at the present time. In order to develop an appropriate tissue-engineered substitute for the ACL that will allow regeneration *in vivo*, a suitable animal model is required. In this study, the fabrication of a biodegradable engineered graft is described, as is its *in vivo* implantation using a reproducible model of ACL reconstruction in an athymic rat. This model can be utilized to evaluate different tissue-engineered ACL grafts composed of various biomaterials, including cellular grafts and those with incorporated growth factors.

In this particular study, we tested an acellular, electrospun polycaprolactone graft with aligned fibers. Previous studies of tissue engineered ligament reconstruction have implanted braided or extruded grafts made of a variety of materials including silk, PLLA, and polyurethane²⁷⁻²⁹. None of these materials resulted in both successful integration of the graft and recapitulation of the mechanical properties of ACL⁷. While many polymers have the potential for use in ligament reconstruction, this study investigated PCL because it is biologically inert, non-toxic, degrades slowly *in vivo*, and is easily manufactured into a desired conformation³⁰. PCL is also mechanically robust and shows little plastic deformation under mechanical stress³⁰. Its use has been established in the bone tissue engineering literature as a reliable reservoir for mineralization and type I collagen deposition due to its aligned nanofiber structure when electrospun³¹. Also, it has been shown that the high surface to volume and short diffusion length scale of the small diameter fibers in electrospun PCL mats are favorable for controlled drug delivery and use in tissue engineering³¹.

It was found that the implanted grafts were biocompatible based on a lack of clinical adverse reaction, and facilitated native cell infiltration as seen histologically at 16 weeks post-operatively. We utilized an athymic animal model in this study as it is the first stage of a two-stage project that will eventually utilize human cells implanted with the graft, and an athymic model would reduce concerns regarding rejection of the human cells. The electrospun polymer scaffold facilitated both cell and matrix alignment in the regenerated ACL. As seen in the cross-section of the graft, the majority of the cells were aligned in the direction of the fibers. The implanted grafts showed increased mechanical properties over time. Load to failure of the polymer grafts doubled as compared to the reconstructed ACL immediately postoperatively. While the peak load and stiffness of the PCL graft may seem low in comparison to native ACL, it is important to remember that these results should be viewed in light of the fact that even the current gold standard, autografts or allografts, are not able to achieve the mechanical strength of healthy ACL by 16 weeks postoperatively. For example, Xu *et al.* reported on an ACL autograft in a rabbit model, in which peak load was 20%-35% and stiffness was 23%-36% that of healthy native ACL by 6 months postoperatively³². Additionally, an allograft study in a canine model demonstrated approximately 30% the peak load and 40% the stiffness of native ACL by 30 weeks postoperatively³³.

While it is outside the scope of this paper, many other analyses may be performed to evaluate graft quality after use of this animal model. This includes but is not limited to bioluminescent imaging or X-rays and CT scans *in vivo*, and a multitude of stains and assays such as immunohistochemistry for collagen markers or inflammatory markers. For instance, we previously published results on the quantification of aligned collagen fibers using picrosirius red staining after implantation of electrospun PCL scaffolds implanted in this animal model²⁶.

Potential limitations of this study include the choice of the animal model itself. The inherent differences in anatomy and gait in the quadrupedal rat compared to bipedal humans mean that the biomechanics of the ACL do vary and that translation of clinical parameters between models should be done with knowledge of these limitations. However, this issue is common in animal studies and does not negate the importance or translational potential of this research.

There has been interesting research on post-operative protocols for rat ACL reconstruction using autograft that may be applied to our model for engineered ACL replacements in the future. External fixation devices have been used to immobilize rats post-operatively in order to allow improved tendon-bone healing in a tendon autograft model¹⁹. Additionally, it has been shown that delayed cyclic loading, such as with the flexion-extension device described by Stasiak *et al.*³⁴, may further enhance autograft incorporation²⁰. However, it has also been shown that short duration low magnitude cyclic loading can also cause increased inflammation and decreased bone formation at the bone-tendon interface³⁵. Further investigation must be conducted to evaluate the applicability of these findings to an electrospun, polymer-based ACL replacement, as such a graft would have weaker initial mechanical properties than a tendon allograft.

The present study has developed a model of ACL reconstruction with an acellular electrospun graft in an athymic rat, based off modifications of a previously described rat autograft model¹⁷⁻²². We demonstrated the elaboration of dense-aligned collagen throughout the graft with a concurrent improvement of load to failure of the graft over time. This study also provides proof of concept for employing this model in the future to evaluate various tissue-engineered grafts for ACL reconstruction. In particular, the athymic rat allows for the seeding of xenogeneic donor cells.

Disclosures

The authors declare that they have no competing financial interests.

Acknowledgements

The authors would like to thank Gabriel Arom and Michael Yeranorian for their technical contributions to earlier iterations of this project. This project was funded by the OREF Clinician Scientist Training Grant (NL), H H Lee Surgical Research Grant (NL), Veterans Administration BLR&D Merit Review 1 I01 BX00012601 (DM) and Musculoskeletal Transplantation Foundation Young Investigator Award (FP).

References

- Fetto, J. F., Marshall, J. L. The natural history and diagnosis of anterior cruciate ligament insufficiency. *Clin Orthop Relat Res.* (147), 29-38 (1980).
- Kim, Y. M., Lee, C. A., Matava, M. J. Clinical results of arthroscopic single-bundle transtibial posterior cruciate ligament reconstruction: a systematic review. *Am J Sports Med.* **39**, (2), 425-434 (2011).
- Andersson, C., Odensten, M., Gillquist, J. Knee function after surgical or nonsurgical treatment of acute rupture of the anterior cruciate ligament: a randomized study with a long-term follow-up period. *Clin Orthop Relat Res.* (264), 255-263 (1991).
- Klimkiewicz, J. J., Petrie, R. S., Harner, C. D. Surgical treatment of combined injury to anterior cruciate ligament, posterior cruciate ligament, and medial structures. *Clin Sports Med.* **19**, (3), 479-492 (2000).
- Petrigliano, F. A., McAllister, D. R., Wu, B. M. Tissue engineering for anterior cruciate ligament reconstruction: a review of current strategies. *Arthroscopy.* **22**, (4), 441-451 (2006).
- Groot, J. H., *et al.* Use of porous polyurethanes for meniscal reconstruction and meniscal prostheses. *Biomaterials.* **17**, (2), 163-173 (1996).
- Leong, N. L., Petrigliano, F. A., McAllister, D. R. Current tissue engineering strategies in anterior cruciate ligament reconstruction. *J Biomed Mater Res A.* **102**, (5), 1614-1624 (2014).
- Duling, R. R., Dupaux, R. B., Katsube, N., Lannutti, J. Mechanical characterization of electrospun polycaprolactone (PCL): a potential scaffold for tissue engineering. *J Biomech Eng.* **130**, (1), 011006 (2008).
- Shao, Z., *et al.* Polycaprolactone electrospun mesh conjugated with an MSC affinity peptide for MSC homing in vivo. *Biomaterials.* **33**, (12), 3375-3387 (2012).
- Tillman, B. W., *et al.* The in vivo stability of electrospun polycaprolactone-collagen scaffolds in vascular reconstruction. *Biomaterials.* **30**, (4), 583-588 (2009).
- Wise, S. G., *et al.* A multilayered synthetic human elastin/polycaprolactone hybrid vascular graft with tailored mechanical properties. *Acta Biomater.* **7**, (1), 295-303 (2011).
- Vargel, I., Korkusuz, P., Menceloğlu, Y. Z., Pişkin, E. In vivo performance of antibiotic embedded electrospun PCL membranes for prevention of abdominal adhesions. *J Biomed Mater Res B Appl Biomater.* **81**, (2), 530-543 (2007).
- Cao, H., McHugh, K., Chew, S. Y., Anderson, J. M. The topographical effect of electrospun nanofibrous scaffolds on the in vivo and in vitro foreign body reaction. *J Biomed Mater Res A.* **93**, (3), 1151-1159 (2010).
- Joshi, V. S., Lei, N. Y., Walther, C. M., Wu, B., Dunn, J. C. Macroporosity enhances vascularization of electrospun scaffolds. *J Surg Res.* **183**, (1), 18-26 (2013).
- Pham, Q. P., Sharma, U., Mikos, A. G. Electrospun poly(epsilon-caprolactone) microfiber and multilayer nanofiber/microfiber scaffolds: characterization of scaffolds and measurement of cellular infiltration. *Biomacromolecules.* **7**, (10), 2796-2805 (2006).
- Vaz, C. M., van Tuijl, S., Bouten, C. V., Baaijens, F. P. Design of scaffolds for blood vessel tissue engineering using a multi-layering electrospinning technique. *Acta Biomater.* **1**, (5), 575-582 (2005).
- Kawamura, S., Ying, L., Kim, H. J., Dymybil, C., Rodeo, S. A. Macrophages accumulate in the early phase of tendon-bone healing. *J Orthop Res.* **23**, (6), 1425-1432 (2005).
- Hays, P. L., *et al.* The role of macrophages in early healing of a tendon graft in a bone tunnel. *J Bone Joint Surg Am.* **90**, (3), 565-579 (2008).
- Dagher, E., *et al.* Immobilization modulates macrophage accumulation in tendon-bone healing. *Clin Orthop Relat Res.* **467**, (1), 281-287 (2009).
- Bedi, A., *et al.* Effect of early and delayed mechanical loading on tendon-to-bone healing after anterior cruciate ligament reconstruction. *J Bone Joint Surg Am.* **92**, (14), 2387-2401 (2010).
- Bedi, A., Kawamura, S., Ying, L., Rodeo, S. A. Differences in tendon graft healing between the intra-articular and extra-articular ends of a bone tunnel. *HSS J.* **5**, (1), 51-57 (2009).
- Fu, S. C., *et al.* Effect of graft tensioning on mechanical restoration in a rat model of anterior cruciate ligament reconstruction using free tendon graft. *Knee Surg Sports Traumatol Arthrosc.* **21**, (5), 1226-1233 (2013).

23. Fan, H., Liu, H., Wong, E. J., Toh, S. L., Goh, J. C. In vivo study of anterior cruciate ligament regeneration using mesenchymal stem cells and silk scaffold. *Biomaterials*. **29**, (23), 3324-3337 (2008).
24. Landis, J. R., Koch, G. G. The measurement of observer agreement for categorical data. *Biometrics*. **33**, (1), 159-174 (1977).
25. Joshi, S. M., Mastrangelo, A. N., Magarian, E. M., Fleming, B. C., Murray, M. M. Collagen-platelet composite enhances biomechanical and histologic healing of the porcine anterior cruciate ligament. *Am J Sports Med*. **37**, (12), 2401-2410 (2009).
26. Leong, N. L., *et al.* In vitro and in vivo evaluation of heparin mediated growth factor release from tissue-engineered constructs for anterior cruciate ligament reconstruction. *J Orthop Res*. **10**, (2014).
27. Seo, Y. K., *et al.* Increase in cell migration and angiogenesis in a composite silk scaffold for tissue-engineered ligaments. *J Orthop Res*. **27**, (4), 495-503 (2009).
28. Freeman, J. W., Woods, M. D., Laurencin, C. T. Tissue engineering of the anterior cruciate ligament using a braid-twist scaffold design. *J Biomech*. **40**, (9), 2029-2036 (2007).
29. Bashur, C. A., Shaffer, R. D., Dahlgren, L. A., Guelcher, S. A., Goldstein, A. S. Effect of fiber diameter and alignment of electrospun polyurethane meshes on mesenchymal progenitor cells. *Tissue Eng Part A*. **15**, (9), 2435-2445 (2009).
30. Dash, T. K., Konkimalla, V. B. Poly-ε-caprolactone based formulations for drug delivery and tissue engineering: A review. *J Control Release*. **158**, (1), 15-33 (2012).
31. Yoshimoto, H., Shin, Y. M., Terai, H., Vacanti, J. P. A biodegradable nanofiber scaffold by electrospinning and its potential for bone tissue engineering. *Biomaterials*. **24**, (12), 2077-2082 (2003).
32. Xu, Y., Ao, Y. F. Histological and biomechanical studies of inter-strand healing in four-strand autograft anterior cruciate ligament reconstruction in a rabbit model. *Knee Surg Sports Traumatol Arthrosc*. **17**, (7), 770-777 (2009).
33. Shino, K., *et al.* Replacement of the anterior cruciate ligament by an allogeneic tendon graft. An experimental study in the dog. *J Bone Joint Surg Br*. **66**, (5), 672-681 (1984).
34. Stasiak, M. E., *et al.* A novel device to apply controlled flexion and extension to the rat knee following anterior cruciate ligament reconstruction. *J Biomech Eng*. **134**, (4), 041008 (2012).
35. Brophy, R. H., *et al.* Effect of short-duration low-magnitude cyclic loading versus immobilization on tendon-bone healing after ACL reconstruction in a rat model. *J Bone Joint Surg Am*. **93**, (4), 381-393 (2011).